A Temporal Coherence Study of Quantum-Dot/Dash Broadband Lasers and Superluminescent Diodes

Clara E. Dimas, *Student Member, IEEE*, Chee-Loon Tan, *Student Member, IEEE*, Hery Susanto Djie, *Member, IEEE*, Alastair D. McAulay, *Senior Member, IEEE*, and Boon-Siew Ooi, *Senior Member, IEEE*

***Abstract*—The temporal coherence functions of InGaAs–GaAs quantum-dot (QD) and InAs–InGaAlAs quantum-dash (Qdash) superluminescent diodes (SLDs) and broadband laser diodes (BLDs) are reported. Using an optical fiber-based spectral interferometer, the fabricated devices were shown to yield low coherence lengths of 4.00–12.29 μm and 33.48–74.56 μm for SLD and BLD devices, respectively. In addition, there were negligible secondary coherencies indicating that these devices have the potential for use in low coherent interferometric systems.**

***Index Terms*—Quantum-dash (Qdash), quantum-dot (QD), semiconductor laser, superluminescent diode (SLD), temporal coherence.**

I. Introduction

BROAD spectral bandwidth sources in the near-infrared wavelength regime are highly desirable for sensing and imaging systems based on low coherent interferometry applications such as optical coherence tomography (OCT) [1]–[3]. In OCT, the axial resolution is inversely proportional to the bandwidth of the light source and the sensitivity is directly proportional to the optical power [1]. Superluminescent diodes (SLDs) and broadband laser diodes (BLDs) based on quantum-dot (QD) and quantum-dash (Qdash) semiconductor nanostructures have demonstrated to be compact broad bandwidth and high emission power light sources highly favorable for low coherent interferometry applications [4]–[8]. The broad, continuous emission spectra from these light sources can be obtained by engineering the optical gain characteristics of naturally inhomogeneous QD/Qdash media to produce an overlap emission from multiple quantum confined states. In addition, the characteristic Gaussian-like low ripple emission makes these devices particularly more attractive for OCT than other bulky alternative broadband sources. Image artifacts and masking can result from significant spectral dips and modulations [9].

While there have been many reports utilizing an OSA to characterize broadband light sources, the important corresponding temporal coherence function, which impacts resolution, signal quality and noise levels in OCT, is still understudied. Thus far, only few measurements of the coherence function of SLDs have been reported [10], [11]. In this letter, we report the first measurement of the temporal coherence function in InGaAs–GaAs QD and InAs–InGaAlAs Qdash based SLDs and BLDs. The relevance of these devices for low coherent interferometric systems has also been evaluated.

Manuscript received November 21, 2008; revised February 13, 2009. First published March 16, 2009; current version published May 08, 2009. This work was supported in part by the National Science Foundation (NSF) under Grant 0725647, in part by the U.S. Army Research Laboratory, in part by the Commonwealth of Pennsylvania, and in part by the Department of Community and Economic Development.

C. E. Dimas, C.-L. Tan, A. McAulay, and B.-S. Ooi are with the Electrical and Computer Engineering Department and the Center for Optical Technologies, Lehigh University, Bethlehem, PA 18015 USA (e-mail: cdimas@lehigh.edu; clt206@lehigh.edu; adm5@lehigh.edu; bsooi@ieee.org).

H. S. Djie is with the JDS Uniphase Corp., San Jose, CA 95134 USA (e-mail: hery@ieee.org).

Color versions of one or more of the figures in this letter are available online at http://ieeexplore.ieee.org.

Digital Object Identifier 10.1109/LPT.2009.2016575

Fig. 1. Schematic of a fiber-based spectral interferometer consisting of a broadband light source coupled into a tapered SMF, a 2 × 2 fiber splitter, two fixed mirrors, and an OSA for signal detection.

II. Measurement Setup

An optical fiber based Michelson interferometer system was setup to generate the coherence function from a spectral interferogram. Unlike a time-domain interferometer, a spectral interferometer does not require a moving reference mirror. In a spectral interferometer, a single broadband depth scan will encode the origin of backscattered light relative to the distance of a parallel arm into the frequency spacing of spectral fringes [1]. Fig. 1 shows a spectral domain fiber-based interferometer consisting of a broadband source, a 2 × 2 single-mode fiber (SMF) splitter, gold mirrors, and an optical spectrum analyzer (OSA). The source is split into two paths (Arm_1 and Arm_2) that are reflected and combined forming the interference signal. The spectral interferogram is then detected by an OSA, with a wavelength resolution of 0.05 nm.

This simple coherence measurement system has several advantages. Optical feedback to the light source is minimized with an antireflection-coated tapered SMF, which couples light from the unpackaged SLD/BLD. Fixed mirrors are placed in contact with Arm_1 and Arm_2 terminals to increase back reflections and to minimize dispersion. All-optical signals are confined in unstressed fiber, thus forgoing needing polarization matching components.

Since the optical pathlength difference (OPD) between Arm_1 and Arm_2 is greater than the coherence length l_c, interference fringes are evident from a spectral interferogram, unlike a temporal domain interferogram which requires the OPD to be much less than l_c. This can be formulated as [10]

$$I(t) = I_1(t) + I_2(t) + 2\,|\alpha^*\gamma|\, e^{-\mathrm{OPD}/l_c} \cos(\beta_o \mathrm{OPD}) \quad (1)$$

where I is the interference intensity; I_1 and I_2 are the intensities of the optical fields of Arm_1 and Arm_2, respectively; α and γ are the coupling ratios of each arm; β_o is the propagation constant

calculated at the center wavelength. Equation (1) shows that the interference visibility is governed by the $\exp[-\mathrm{OPD}/l_c]$, which is the envelope of the normalized cross-correlation function between I_1 and I_2 subject to OPD. Consequently, the interference fringes will be greater if OPD $> l_c$ in the frequency domain but diminishes in the spatial domain due to the inverse nature of the two domains [12]. Since the number of fringes increases as the OPD increases, the upper limit of OPD is defined by the OSA resolution. Hence a 2×2 fiber splitter with a proper OPD is essential in this measurement setup.

The coherence length l_c of a light source is found experimentally by measuring the full-width at half-maximum (FWHM) of the coherence function in terms of distance delay. The temporal coherence function is generated by taking the following steps: 1) subtract $S_o(\lambda)$ from $S(\lambda)$, where $S(\lambda)$ is the spectral interferogram, and $S_o(\lambda)$ is the input source spectrum; 2) convert wavelength to evenly sampled wave numbers via interpolation; 3) take the inverse Fourier transform of the spectral interferogram; 4) convert wavenumber to time delay and OPD [13]. For a light source with a Gaussian emission spectrum, l_c can be calculated from the following equation [1]:

$$l_c = \frac{2\ln(2)}{\pi n_g}\frac{\lambda^2}{\Delta\lambda} \tag{2}$$

where λ_o is the center wavelength, $\Delta\lambda$ is the FWHM of the source, and n_g is the group refractive index.

SLDs and BLDs were fabricated on InGaAs–GaAs QD and InAs–InGaAlAs Qdash material in the form of a standard ridge waveguide structure with a broad-area photon absorber (PA) and gain guided structure, respectively. The epitaxial layers, growth conditions and geometrical structures of these devices have been described elsewhere [4]–[8].

III. Results and Discussion

InGaAs–GaAs QD SLDs [4] and InAs–InGaAlAs Qdash SLDs [6] were tested at 20 °C under continuous-wave operation at maximum current injections of 3.00 and 15.83 kA/cm^2, respectively. The output power versus current (L–I) curves showed a typical superlinear characteristic under moderate current injection followed by a thermal roll-off. The corresponding maximum optical powers were 10 and 100 μW for the QD and the Qdash devices, respectively. The low emission power is due to the small active volume as it is an index-guided 4-μm-wide (<600 m long) ridge waveguide. The theoretical and experimental l_c in fiber for the QD SLD is 2.75 and 2.74 μm, respectively, while the calculated and measured l_c of the Qdash SLD is 9.88 and 8.42 μm, respectively. The corresponding l_c in air is 4.00 and 12.29 μm, for the QD and Qdash SLDs, respectively. Fig. 2 shows the coherence function versus distance delay and the inset illustrates $S(\lambda)$ and $S_o(\lambda)$. The physical pathlength difference between Arm$_1$ and Arm$_2$, l, which is defined as $l = \mathrm{OPD}/(2n_g)$, is ~250 μm as shown in Fig. 2 at the peak of the coherence function.

In addition to the coherence length l_c and OPD, the coherence function also reveals the impact of sidelobes on the l_c and the significance of far range peaks on sensitivity. Secondary coherence subpeaks can appear in the short range if a prominent spectral dip occurs between multiple-state excitation peaks. Since the QD and Qdash SLDs tested have small spectral dips (<1 dB), secondary sidelobes were suppressed by more than 9 and 11 dB, respectively, without increasing the coherence

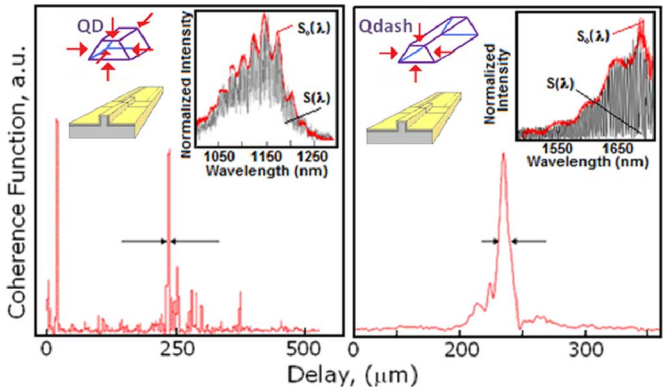

Fig. 2. (a) Temporal coherence functions of the InGaAs–GaAs QD and (b) the InAs–InGaAlAs Qdash SLDs taken at 20 °C. The insets delineate the intensity of the spectral interferogram and the input spectrum.

length. The QD and Qdash SLD samples tested have active lengths L of 500 and 600 μm, respectively. In terms of far range peaks, there are no parasitic subpeaks appearing at $2n_{\mathrm{eff}}L$, where n_{eff} is the effective refractive index of the optical mode. At this distance, subpeaks can occur due to Fabry–Pérot modulation [1]. The two SLDs tested exhibited low spectral modulation (<0.5 dB); a result of effective absorption of photon in the integrated PA section.

InGaAs–GaAs QD [5] and InAs–InGaAlAs Qdash BLDs [7] were tested at 20 °C under pulsed current operation (0.4% duty cycle with a pulse width of 2 μs) at maximum current injections of 10.69 and 12.00 kA/cm^2, respectively. The L–I curves yield threshold currents for the QD and Qdash lasers at 3.9 and 3.3 kA/cm^2, with the corresponding maximum output power of 217 mW and 328 mW, respectively. Under stimulated emission, these gain-guided 50-μm broad-area devices provide greater emission power than the SLDs. To minimize spectral noise, ten spectral scans were averaged per dataset. To further validate the experimental setup and data acquisition trigger, spectral modulations were compared to fitted data sets based on the input spectrum using a frequency domain version of (1) [14]

$$S(\upsilon) = S_o(\upsilon)\left[1 + V_o\cos\left(2\pi\frac{\mathrm{OPD}}{\lambda}\right)\right] \tag{3}$$

where $S(\upsilon)$ is the spectral interferogram, $S_o(\upsilon)$ is the input spectrum, and V_o is the fringe visibility. As can be seen from Fig. 3, the measured data matches well (less than 5% error) with the fit data set for both BLDs. The low fit error and high visibility also indicates that stress induced birefringence due to a polarization mismatch between Arm$_1$ and Arm$_2$ is minimal.

The coherence function, as shown in Fig. 4, was obtained for the QD BLDs and Qdash BLDs with cavity lengths of 800 and 600 μm, respectively. Theoretically, the l_c in fiber for the QD BLD is 23.05 μm, experimentally it is 22.93 μm; whereas the calculated and measured l_c for the Qdash BLD is 48.39 and 51.07 μm, respectively. From the measured signals, the l_c in air is 33.48 and 74.56 μm, for the QD and Qdash BLDs, respectively. Both short- and long-range subpeaks in both QD and Qdash BLDs were suppressed more than 8 and 16 dB, respectively. These results confirm the Gaussian-like nature of the emission from the naturally inhomogeneous QDs and Qdashes and multiple excitation states. Such spectra generated coherence

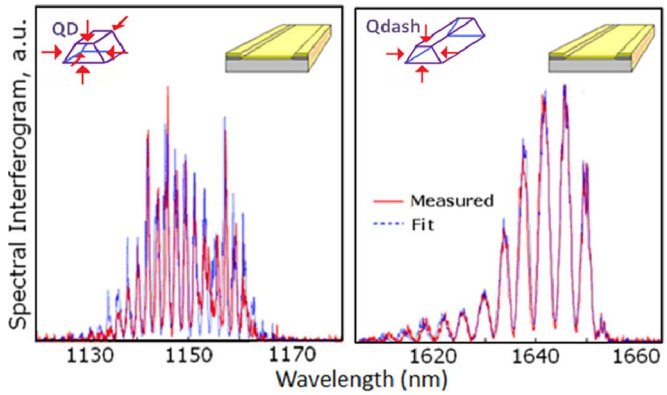

Fig. 3. Spectral interferograms measured and calculated fit based on the input spectrum for InGaAs–GaAs QD and InAs–InGaAlAs Qdash based BLDs.

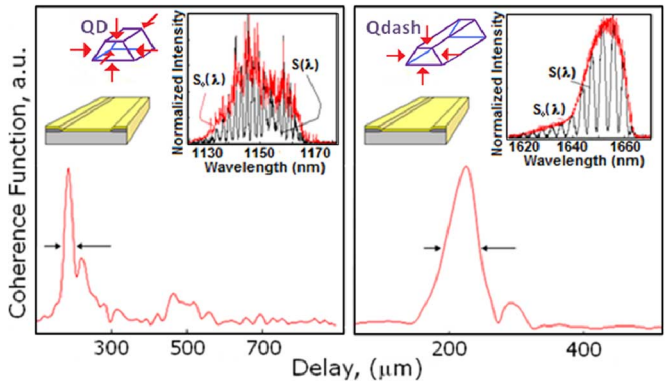

Fig. 4. Temporal coherence functions of the InGaAs–GaAs QD and InAs–InGaAlAs Qdash BLDs taken at 20 °C. The insets delineate the intensity of the spectral interferogram and the input spectrum.

lengths close (to within 0.5% and 5.5%, respectively) to the theoretical value, which results in less error than other published SLD results [10], [11]. The variation may be attributed to spectral phase and amplitude fluctuations of the nonoptimized structure.

This is the first reported temporal coherence measurement of the recently developed BLDs. Besides the relatively narrow spectral bandwidth from the present devices, our measurements show that the other coherence function characteristics are favorable for low coherent interferometry. Although diode pumped and external cavity laser sources as well as coupled SLDs achieve axial resolutions below 3 μm in tissue [16], our SLDs and BLDs provide a much more compact and less complex solution, consisting of only a single optical device and single driver. The spectral bandwidth of BLD devices can be further broadened to obtain a lower coherence length of a few of microns by adopting the chirped QD/Qdash configuration [11] and/or spatial bandgap engineering via the intermixing technology [15].

IV. Conclusion

We successfully measured and evaluated the temporal coherence function of InGaAs–GaAs QD and InAs–InGaAlAs Qdash based SLDs and BLDs using an optical fiber-based spectral interferometer. In comparing the low coherency of SLDs with BLDs, it is evident that even though BLDs do not produce low ripple spectra compared to SLDs fabricated on similar type of structures, the corresponding coherence function is free of significant sidelobes and subpeaks which would otherwise introduce significant image artifacts and detracted from the axial resolution. Our results confirm that both SLD and BLD based on QD and Qdash nanostructures are promising for low coherent applications such as OCT.

References

[1] A. F. Fercher, W. Drexler, C. K. Hitzenberger, and T. Lasser, "Optical coherence tomography—Principles and applications," *Rep. Prog. Phys.*, vol. 66, pp. 239–303, Jan. 2003.

[2] T. H. Ko, D. C. Adler, J. G. Fujimoto, D. Mamedov, V. Prokhorov, V. Shidlovski, and S. Yakubovich, "Ultrahigh resolution optical coherence tomography imaging with a broadband superluminescent diode light source," *Opt. Express*, vol. 12, no. 10, pp. 2112–2119, Apr. 2004.

[3] W. Jung, J. Zhang, J. Chung, P. Wilder-Smith, M. Brenner, J. S. Nelson, and Z. Chen, "Advances in oral cancer detection using optical coherence tomography," *IEEE Sel. Top. Quant. Elect.*, vol. 11, no. 4, pp. 811–817, Aug. 2005.

[4] C. E. Dimas, H. S. Djie, and B. S. Ooi, "Superluminescent diodes using quantum dots superlattice," *J. Cryst. Growth*, vol. 288, pp. 153–156, Feb. 2006.

[5] H. S. Djie, B. S. Ooi, X. -M. Fang, Y. Wu, J. M. Fastenau, W. K. Liu, and M. Hopkinson, "Room temperature broadband emission of InGaAs/GaAs quantum-dots laser," *Opt. Lett.*, vol. 32, pp. 44–46, Jan. 2007.

[6] H. S. Djie, C. E. Dimas, and B. S. Ooi, "Wideband quantum-dash-in-well superluminescent diode at 1.6 μm," *IEEE Photon. Technol. Lett.*, vol. 18, pp. 1747–1749, Aug. 2006.

[7] H. S. Djie, C. L. Tan, B. S. Ooi, J. C. M. Hwang, X. -M. Fang, Y. Wu, J. M. Fastenau, W. K. Liu, G. T. Dang, and W. H. Chang, "Ultra-broad stimulated emission from quantum-dash laser," *Appl. Phys. Lett.*, vol. 91, no. 11, p. 111116, Sep. 2007.

[8] B. S. Ooi, H. S. Djie, Y. Wang, C. L. Tan, J. C. M. Hwang, X. M. Fang, J. M. Fastenau, A. W. K. Liu, G. T. Dang, and W. H. Chang, "Quantum dashes on InP substrate for broadband emitter applications," *IEEE J. Sel. Top. Quantum Electron.*, vol. 14, pp. 1230–1238, Aug. 2008.

[9] J. Goodman, *Statistical Optics*. New York: Wiley, 1985.

[10] D. S. Mamedov, V. V. Prokhorov, and S. D. Yakubovich, "Super-broadband high-power superluminescent diode emitting at 920 nm," *Quantum Electron.*, vol. 33, no. 6, pp. 471–473, Mar. 2003.

[11] M. Rossetti, L. L. Li, A. Markus, A. Fiore, L. Occhi, C. Velez, S. Mikhrin, I. Krestnikov, and A. Kovsh, "Characterization and modeling of broad spectrum InAs-GaAs quantum-dot superluminescent diodes emitting at 1.2–1.3 μm," *IEEE J. Quant. Elect.*, vol. 43, no. 8, pp. 676–686, Aug. 2007.

[12] H. K. Teng, C. N. Chang, and K. C. Lang, "Determination of path length difference by low coherence interference spectrum," *Opt. Laser Eng.*, vol. 42, pp. 437–446, Oct. 2004.

[13] K. E. Braun, J. D. Boyer, M. H. Henderson, D. F. Katz, and A. Wax, "Label-free measurement of microbicidal gel thickness using low-coherence interferometry," *J. Biomed. Opt.*, vol. 11, pp. 020504–020504, May 2006.

[14] M. Jedrzejewska-Szczerska, R. Bogdanowicz, M. Gnyba, R. Hypszer, and B. B. Kosmowski, "Fiber-optic temperature sensor using low-coherence interferometry," *Eur. Phys. J. Special Topics*, vol. 154, pp. 107–111, Dec. 2008.

[15] C. L. Tan, H. S. Djie, Y. Wang, C. E. Dimas, V. Hongpinyo, Y. H. Ding, and B. S. Ooi, "Wavelength tuning and emission width widening of ultrabroad quantum dash interband laser," *Appl. Phys. Lett.*, vol. 93, no. 11, p. 111101, Sep. 2008.

[16] A. M. Zysk, F. T. Nguyen, A. L. Oldenburg, D. L. Marks, and S. A. Boppart, "Optical coherence tomography: A review of clinical development from bench to bedside," *J. Biomed. Opt.*, vol. 12, no. 5, pp. 51403–51424, Sep. 2007.